



A Method to Correct the Raw Doppler Observations for GNSS Velocity Determination

Kaifei He, Tianhe Xu, Christoph Förste, Zhenjie Wang, Qiang Zhao, and Yongseng Wei

Abstract

In the application of GNSS in the velocity determination, it is often the case that some GNSS receivers give an opposite sign for the raw Doppler observations which do not correspond to the real Doppler shift. This is caused by different methods of the GNSS signal processing in different GNSS receivers. If the velocities of kinematic platforms are calculated by using raw Doppler observations from the GNSS receiver directly, the directions of the estimated velocities may be reversed, and the value of the velocity is wrong with respect to the actual movement. This would lead to incorrect results, and unacceptable for research and applications. To overcome this problem, a new method of sign correction for raw Doppler observations is proposed in this study. This algorithm constructs a correction function based on the GNSS carrier-phase-derived Doppler observations. To test this approach, GNSS data of GEOHALO airborne gravimetric missions have been used. The results show that the proposed method, which is straightforward and practical, can produce the correct velocity for a kinematic platform in any case, independent of the internal hardware structure and the specific way of the signal processing of the GNSS receivers in question.

Keywords

Doppler observation · GNSS · Kinematic platform · Sign correction · Velocity determination

1 Introduction

GNSS is a cost-effective means to obtain reliable and high-precision velocities by exploiting the receiver raw Doppler (RD) and carrier-phase-derived Doppler (CD) measurements (Szarmes et al. 1997). The RD method is the most widely used technique and usually has a cm/s accuracy (Wang and Xu 2011). The CD method consists in differencing

successive carrier phases observations, enables accuracies at the mm/s level (Freda et al. 2015). Since the CD is computed over a longer time span than the raw one, the random noise is averaged and suppressed. Therefore, very smooth velocity estimates in low dynamic environments can be obtained from CD measurements if there are no undetected cycle-slips (Serrano et al. 2004b). However, the functional model of the RD method is stricter than the CD method, and its velocity results are more reliable when a sudden change of the vehicle status occurs, such as braking, turning, and accelerating (Wang and Xu 2011). Thus, the RD method has been investigated here in this study.

In the applications of velocity determination using the RD observations, the sign of Doppler observations from some GNSS receivers is opposite to the real Doppler shift. If the velocity of the kinematic platform is calculated by using the RD observations directly from the GNSS receiver, the direction of the velocity of the kinematic platform will be

K. He (✉) · Z. Wang · Q. Zhao · Y. Wei
College of Oceanography and Space Informatics, China University of Petroleum (East China), Qingdao, China
e-mail: kfhe@upc.edu.cn

T. Xu
Institute of Space Science, Shandong University, Weihai, China

C. Förste
GFZ – German Research Centre for Geosciences, Potsdam, Germany

reverse, and the value of the velocity will be false. Thus, a sign correction method of the RD observations for GNSS velocity determination was studied in this article.

2 Velocity Determination Using GNSS Raw Doppler Observations

The GNSS RD observations, the Doppler shift $D_{r,j}^s$ between the receiver r and the GNSS satellite s at the frequency channel j can be given as (Hofmann-Wellenhof et al. 2008)

$$D_{r,j}^s = f_j^s - f_{r,j}^s = \frac{V_{\rho_r^s}}{c} f_j^s = \frac{V_{\rho_r^s}}{\lambda_j^s} \quad (1)$$

where f_j^s denotes the emitted frequency j of satellite s , $f_{r,j}^s$ is the received frequency j from satellite s , $V_{\rho_r^s}$ is the radial velocity along the range between the receiver r and the satellite s , c means the speed of electromagnetic waves in vacuum and λ_j^s denotes the wavelength. $D_{r,j}^s$ has a negative sign when the receiver and the transmitter move away from each other and a positive sign when they approach each other. Equation (1) for the observed Doppler shift scaled to range rate can be written as

$$V_{\rho_r^s} = \lambda_j^s \cdot D_{r,j}^s = \dot{\rho}_r^s + c \cdot (d\dot{t}_r - d\dot{t}^s) + \dot{T}_r - \dot{I}_{r,j}^s + \varepsilon_{r,j}^s \quad (2)$$

where the derivatives with respect to time are indicated by a dot, $\dot{\rho}_r^s$ means for the geometric range rate between the receiver r and the satellite s , the signs $d\dot{t}^s$ and $d\dot{t}_r$ are the satellite clock drift and receiver clock drift, respectively, \dot{T} and \dot{I} denote the tropospheric and the ionospheric delay rate, respectively, and $\varepsilon_{r,j}^s$ denotes all non-modeled error sources (e.g. multipath error) and the effect of the observational noise. The precise velocity estimation of the kinematic station can be directly obtained by the classic Least-Squares adjustment (Koch 1999), if Doppler observations from more than four GNSS satellites have been measured.

Normally, it is no problem to obtain the velocity information from the GNSS RD observations, but, in the case of some GNSS receivers (such as in the chosen experiments in this paper), the signs of the RD observations are opposite to the real Doppler shift. This phenomenon is caused by different methods of GNSS signal processing in different GNSS receivers. In such situations, the direction of the estimated velocity will be reversed and the value of velocity will be false compared with the actual movement if the velocity of a kinematic platform is calculated by directly using the RD observations from the GNSS receiver. To solve this problem, an algorithm has to be developed to obtain the correct velocity from GNSS RD observations.

3 A New Method of Sign Correction for GNSS Raw Doppler Observations

In order to solve the above-named problem, a correction function is constructed based on the CD observations. Then, the GNSS RD observations will be corrected using the correction function.

3.1 Carrier-Phase-Derived Doppler Observations

The CD observations can be obtained by differencing carrier phase observations in the time domain, normalizing them with the time interval of the differenced observations or by fitting a curve to successive phase measurements, using polynomials of various orders (Serrano et al. 2004a). At present, the first order central difference is one of the most popular methods for obtaining the virtual Doppler observations (Wang and Xu 2011). Based on the fundamental GNSS carrier-phase observation, the CD observation is given by

$$\dot{\phi}_t = \frac{1}{2} \left(\frac{\varphi_{t+\delta t} - \varphi_t}{\delta t} + \frac{\varphi_t - \varphi_{t-\delta t}}{\delta t} \right) = \frac{\varphi_{t+\delta t} - \varphi_{t-\delta t}}{2\delta t} \quad (3)$$

where $\dot{\phi}_t$ (namely the CD observation) denotes the variation rate of the raw carrier phase observations φ_t . Here, the carrier phase observations φ_t should don't have the cycle slip. If the cycle slip exist, these observations φ_t should be omit. t means the observation time and δt denotes the data sample interval.

The resulting observation equation for velocity determination can be expressed as

$$V_{\rho_r^s} = \lambda_j \dot{\phi}_{r,j}^s = \dot{\rho}_r^s + c \cdot (d\dot{t}_r - d\dot{t}^s) + \dot{T}_r - \dot{I}_{r,j}^s + \varepsilon_{r,j}^s \quad (4)$$

Here, the CD observation $\dot{\phi}_{r,j}^s$ of Eq. (4) has a similar function as the RD $D_{r,j}^s$ of Eq. (2). Thus, this relationship can be used to solve the problem as already stated in our previous letter.

3.2 Construction of the Sign Correction Function

The RD observations should, of course, have the same sign as the CD observations. Therefore, a sign correction function $f(j)$ is constructed as

$$f(j) = \begin{cases} 1, & \text{if } (D_{r,j}^s \cdot \dot{\phi}_t > 0) \\ -1, & \text{if } (D_{r,j}^s \cdot \dot{\phi}_t < 0) \end{cases} \quad (5)$$

Here, if the RD observation $D_{r,j}^s$ has the same sign as the CD observation $\dot{\varphi}_l$, the value of the sign correction function $f(j)$ will be +1. Otherwise, the value of the sign correction function $f(j)$ will be -1 when the RD observation $D_{r,j}^s$ has a different sign than the CD shift $\dot{\varphi}_l$. In this correction function, the CD observations were calculated by Eq. (3), but do not need to be calculated for all epochs, and just several epochs at the beginning are enough, such as the first 10 epochs (here, should be omitted the epochs that cycle slip occurrence).

3.3 Correction Method for the GNSS Raw Doppler Observations

After constructing the sign correction function, the GNSS RD observations can be corrected by

$$D_{r,j,new}^s = f(j) \cdot D_{r,j}^s \quad (6)$$

where the GNSS RD observations $D_{r,j}^s$ have been modified by the sign correction function $f(j)$. If the RD observations $D_{r,j}^s$ has another sign than the CD observations $\dot{\varphi}_l$, their sign will be changed by applying this new method using Eq. (6). Then, the corrected Doppler observation $D_{r,j,new}^s$ can be used for the GNSS velocity determination. To illustrate the new method of sign correction, one example is given in the following.

4 Experiments and Analysis

To investigate this new method, the GNSS data of the airborne gravimetry campaign GEOHALO mission over Italy 2012 on June 6, 2012 (He et al. 2016) were chosen for testing. The selected kinematic station was AIR5 at the front part of the HALO aircraft. The station REF6, installed by GFZ next to the runway of the German Aerospace Centre (DLR) airport in Oberpfaffenhofen, Germany, was selected as the reference station. The GNSS receiver types of AIR5 and REF6 were both JAVAD TRE_G3T DELTA. The trajectory of the HALO aircraft on June 6, 2012 and the position of the selected reference station REF6 are shown in Fig. 1. The selected data contain GLONASS and GPS observations with a sampling rate of 1 Hz.

The HALO_GNSS software (He 2015) was used for the GNSS data processing. The calculated trajectory of the HALO aircraft is shown in Fig. 2 as latitude, longitude and height components, respectively. The two significant humps on the height curve correspond to crossing the Alps. In order to investigate the capability of the proposed new approach, two experimental figures were designed as follows.

Figure 3 GNSS velocity determination using the RD observations directly without any correction. The velocity

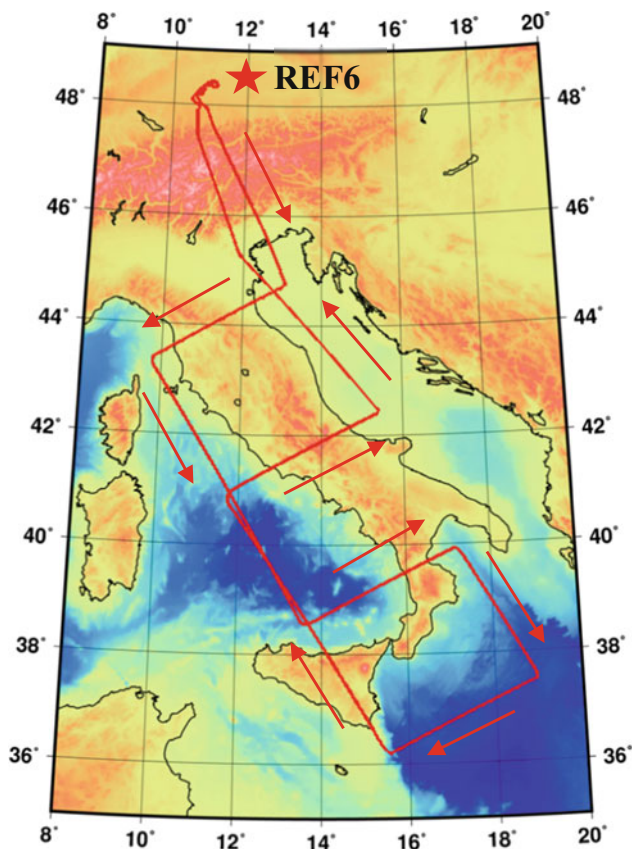


Fig. 1 HALO aircraft flight trajectory on June 6, 2012 and the location of the selected reference station REF6

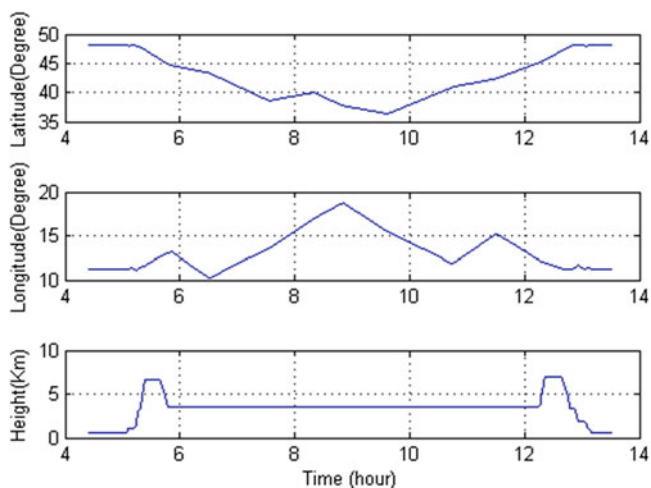


Fig. 2 Components of the flight trajectory of the HALO aircraft on June 6, 2012

results are shown in Fig. 3 as north, east and up components, respectively. The incorrect velocity results can be found in Fig. 3 compared with the trajectory components in Fig. 2. For instance, the latitude component of the trajectory of the HALO aircraft at nearly GPST 10:00 was increasing, and

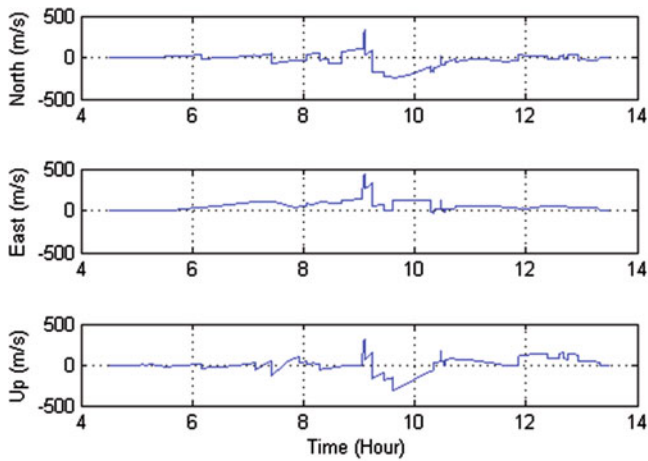


Fig. 3 Velocity components of HALO aircraft calculated from GNSS RD observations

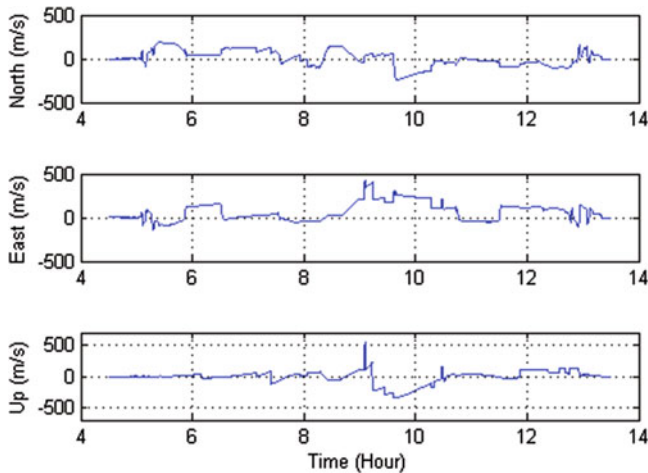


Fig. 4 Difference between velocity results calculated by the RD and CD

its longitude component was decreasing in Fig. 2. Thus, the north component of velocity should be positive and its east component negative, but the corresponding velocities were negative in the north component and positive in the east component in Fig. 3 at that time. Therefore, the direction of the calculated velocity of the HALO aircraft were reversed.

To analyze the value of this results, the velocity results, calculated by CD were used as “true value” to compare with the results of Fig. 3. The difference of the velocity results calculated by CD and RD are plotted in Fig. 4 and its statistic results given in Table 1. It is shown that the value of velocity results of Fig. 3 were false with respect to the actual movement if the velocity is calculated by directly using the RD observations from the GNSS receiver.

Figure 5 GNSS velocity determination using the RD observation corrected by the proposed approach. The veloc-

Table 1 The statistical results of difference between velocity results calculated by the RD and RD (Unit: m/s)

Figure	Directions	Min	Max	Mean	RMS
1	RD vs. CD				
	North	-246.54	198.11	3.20	93.38
	East	-148.17	432.84	61.19	120.76
2	Corrected RD vs. CD				
	North	-0.15	0.36	0.00	0.01
	East	-0.21	0.33	0.00	0.01
	Up	-0.61	0.43	0.00	0.03

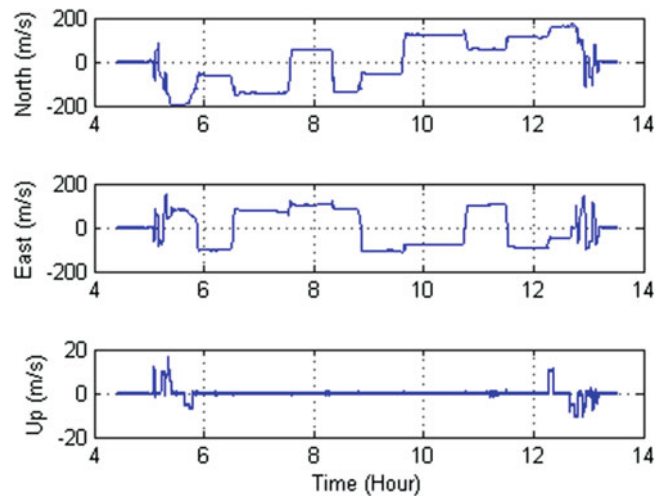


Fig. 5 Velocity components of the HALO aircraft calculated by GNSS RD observations corrected by the proposed approach

ity results are shown in Fig. 5 as north, east and up components, respectively. Compared with Fig. 3, the correct velocity results can be obtained by using the proposed approach. For instance, the corresponding north component of velocity has a positive value and its east component was negative at nearly GPST 10:00 in Fig. 5. Therefore, this example also shows that the proposed approach can correct the error that appeared in Fig. 3.

Compare with mentioned true value, the difference between them is plotted in Fig. 6 and its statistic results given in Table 1 as well. It is shown that the value of velocity results of Fig. 5 correspond with the actual movement if the velocity is calculated by using the corrected RD observations from the GNSS receiver. The reason for the difference between the velocity results calculated by corrected RD and the CD will be discussed in follows.

Normally, it is no problem to obtain the correct velocity information from GNSS RD observations for kinematic platform, but sometimes, such as in the chosen experiments, a problem occurs in the GNSS velocity determination when using the RD observations directly, see Fig. 3. When the proposed method was applied, the results of GNSS velocity determination by using the RD were corrected in such a way

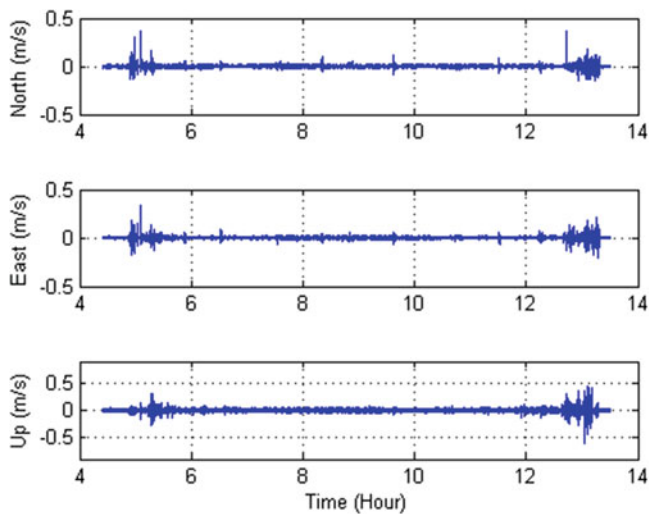


Fig. 6 The difference between velocity results calculated by the corrected RD and CD

that the direction and the magnitude of the estimated velocity corresponded to the actual movement.

The difference between velocity results calculated by corrected RD and the CD, shown as in Fig. 6, have two reasons. The one is the noise of observations that the RD measurements are usually noisier than the CD measurement. The other one is the movement of kinematic platform. The CD observations are average variation rates during a time interval $2\delta t$, see Eq. (3), which are more disturbed than the RD observations $D_{r,j}^s$ at the epoch time t , see Eq. (1). The sudden changes of the state of the HALO aircraft, see Figs. 2 and 5, correspond to the large spikes in Fig. 6. Therefore, the GNSS RD observations are more suitable to calculate the velocity results for highly dynamic platform.

5 Summary

This study focuses on GNSS velocity determination by using RD observations. There could occur a problem when using these observations directly. The direction of the velocity might be reversed and its magnitude false compared with the actual movement since the sign of the RD observations is opposite to the real Doppler shift. The reason for this is different signal processing methods in different types of GNSS receivers. It is hard for users to distinguish between the intrinsic methods of signal processing for every different type of GNSS receiver. Therefore, a new method was

proposed to correct the sign of the GNSS RD observations according to a proposed special sign correction function. To test this approach, GNSS data of GEOHALO airborne gravimetric campaigns have been used. The results show that the proposed method can yield the correct velocity of a kinematic platform in any case, without taking into account the internal structure and means of signal processing of the particular GNSS receiver.

Acknowledgements We express our appreciation to our colleagues of GFZ for their cooperation, discussions and providing GNSS data. This work is supported by the National Natural Science Foundation of China (41604027, 41574013), the financial support by Qingdao National Laboratory for Marine Science and Technology (QNL2016ORP0401), the Key R&D Program of China (2016YFB0501700, 2016YFB0501705), the Shandong Provincial Natural Science Foundation (ZR2016DQ01, ZR2019MD005, ZR2016DM15), the Fundamental Research Funds for the Central Universities of China (18CX02054A) and Source Innovation Plan of Qingdao, China (17-1-1-100-jch).

References

- Freda P, Angrisano A, Gaglione S, Troisi S (2015) Time-differenced carrier phases technique for precise GNSS velocity estimation. *GPS Solutions* 19:335–341
- He K (2015) GNSS kinematic position and velocity determination for airborne gravimetry. PhD thesis (scientific technical report 15/04), GFZ - German Research Centre for Geosciences
- He K, Xu G, Xu T, Flechtner F (2016) GNSS navigation and positioning for the GEOHALO experiment in Italy. *GPS Solutions* 20:215–224. <https://doi.org/10.1007/s10291-014-0430-4>
- Hofmann-Wellenhof B, Lichtenegger H, Wasle E (2008) GNSS—global navigation satellite systems: GPS, GLONASS, Galileo, and more. Springer, Wien
- Koch KR (1999) Parameter estimation and hypothesis testing in linear models. Springer, Wien
- Serrano L, Kim D, Langley RB (2004a) A single GPS receiver as a real-time, accurate velocity and acceleration sensor. Paper presented at the 17th International Technical Meeting of the Satellite Division of the Institute of navigation, Long Beach, CA, USA, September 21–24
- Serrano L, Kim D, Langley RB, Itani K, Ueno M (2004b) A gps velocity sensor: how accurate can it be?—a first look. Paper presented at the ION NTM, San Diego, CA, USA, January 26–28
- Szarmes M, Ryan S, Lachapelle G, Fenton P (1997) DGPS high accuracy aircraft velocity determination using Doppler measurements. Paper presented at the International Symposium on Kinematic Systems (KIS), Banff, AB, Canada, June 3–6
- Wang Q, Xu T (2011) Combining GPS carrier phase and Doppler observations for precise velocity determination. *Sci China Phys Mech Astron* 54:1022–1028

Open Access This chapter is licensed under the terms of the Creative Commons Attribution 4.0 International Licence (<http://creativecommons.org/licenses/by/4.0/>), which permits use, sharing, adaptation, distribution and reproduction in any medium or format, as long as you give appropriate credit to the original author(s) and the source, provide a link to the Creative Commons licence and indicate if changes were made.

The images or other third party material in this chapter are included in the chapter's Creative Commons licence, unless indicated otherwise in a credit line to the material. If material is not included in the chapter's Creative Commons licence and your intended use is not permitted by statutory regulation or exceeds the permitted use, you will need to obtain permission directly from the copyright holder.

